Syntheses and crystal structures of bi- and tri-metallic complexes containing a trioxoosmium(VIII) moiety †

Wa-Hung Leung,*‡,ᵃ Joyce L. C. Chim ᵃ and Wing-Tak Wong ᵇ

ᵃ *Department of Chemistry, The Hong Kong University of Science and Technology, Clear Water Bay, Kowloon, Hong Kong*
ᵇ *Department of Chemistry, The University of Hong Kong, Pokfulam Road, Hong Kong*

Interaction of *cis*-[Pt(dppm)₂(O₃SCF₃)₂] [dppm = bis(diphenylphosphino)methane], *cis*-[Pt(Bupy)(O₃SCF₃)₂] (Bupy = 4-*tert*-butylpyridine), [Ir(CO)(PPh₃)₂(O₃SCF₃)], and [Rh(cod)(OH₂)(OTs)] (cod = cycloocta-1,5-diene, OTs = tosylate) with [NBuⁿ₄][NOsO₃] afforded bimetallic nitrido-bridged complexes *cis*-[Pt(dppm)(NOsO₃)₂] **3**, *trans*-[Pt(Bupy)₂(NOsO₃)₂] **4**, [Ir(CO)(PPh₃)₂(NOsO₃)] **5** and [{Rh(cod)(NOsO₃)}₂] **6**, respectively. Complex **4** crystallises in the *P*1̄ space group with *a* = 7.936(1), *b* = 10.758(2), *c* = 7.738(1) Å, α = 100.02(1), β = 99.75(1), γ = 101.75(1)°, *U* = 622.5(2) Å³ for *Z* = 1. The Pt–N (Os), Os–N and the mean Os–O distances are 1.958(7), 1.681(7) and 1.724 Å, respectively. Complex **5** crystallises in the *P*2₁/*n* space group with *a* = 10.124(1), *b* = 15.564(2), *c* = 22.623(3) Å, β = 100.08(2)°, *U* = 3509.7(7) Å³ for *Z* = 4. The Ir–N, Os–N and the mean Os–O distances are 1.998(7), 1.710(7) and 1.718 Å, respectively. Treatment of [Au(PPh₃)(NOsO₃)] **1** with Ph₃P=NPh gave the *N*-phosphinimine complex [Au(PPh₃){N(=PPh₃)Ph}][NOsO₃] **7**. Complex **7** crystallises in the *P*2₁/*n* space group with *a* = 8.780(1), *b* = 20.781(2), *c* = 20.711(5) Å, β = 91.23(1)°, *U* = 3788.0(9) Å³ for *Z* = 4. The Au–N distance is 2.091(8) Å and the C–N–P angle in the phosphinimine is 127.0(7)°. Reaction of **1** with Bupy led to substitution of Bupy for [NOsO₃] and formation of [Au(PPh₃)(Bupy)][NOsO₃] **8**. Reaction of [Pt(dppf)(O₃SCF₃)Cl] [dppf = 1,1′-bis(diphenylphosphino)ferrocene] with [NBuⁿ₄][NOsO₃] afforded the trimetallic complex [Pt(dppf)(NOsO₃)Cl] **11**. Complex **11** crystallizes in the *P*2₁/*c* space group with *a* = 20.058(2), *b* = 14.899(1), *c* = 23.949(2) Å, β = 114.57(2)°, *U* = 6508(1) Å³ for *Z* = 8. The mean Pt–N, Os–N and Os–O distances are 2.06, 1.66 and 1.67 Å, respectively.

Oxoosmium(VIII) complexes have attracted much attention because of their applications to organic syntheses, particularly dihydroxylation[1] and aminohydroxylation[2] of alkenes by [OsO₄] and [Os(NR)O₃] (R = alkyl), respectively. The significance of these reactions is highlighted by the seminal works of Sharpless and co-workers, who have successfully developed versatile syntheses of optically pure vicinal diols and amino alcohols *via* enantioselective osmium-catalysed dihydroxylation[3] and aminohydroxylation[4] of alkenes, respectively. In an effort to explore new reactivities of oxoosmium(VIII) complexes, we set out to investigate the electronic influence of the substituent on nitride (X) on the reactivity of the imidoosmium(VIII) complex [Os(NX)O₃]. To this end, a series of bimetallic nitrido-bridged trioxoosmium(VIII) complexes of the type [LₙM–N≡OsO₃] (M = electrophilic metal; L = PR₃, CO, *etc.*) are synthesised. Of particular interest are the osmate(VIII) complexes containing square planar platinum(II) and iridium(I) centres, which may promote the reactivities of unsaturated organic substrates with the trioxoosmium(VIII) moiety. We describe here the syntheses and reactivities of some bi- and tri-metallic complexes with a trioxoosmium(VIII) moiety. Preliminary results of this work have been published in a communication.[5]

Experimental

All manipulations were carried out under nitrogen using standard Schlenk techniques. Solvents were purified and distilled prior to use; NMR spectra were recorded on a Bruker ALX 300 spectrometer, chemical shifts (δ) were reported with reference to SiMe₄ (¹H) and H₃PO₄ (³¹P). Infrared spectra (Nujol) were recorded on a Perkin-Elmer 16 PC FT-IR spectrophotometer, mass spectra were obtained on a Finnigan TSQ-7000 spec-

trometer. Cyclic voltammetry was performed with a Princeton Applied Research (PAR) Model 273A potentiostat, the working and reference electrodes were glassy carbon and Ag–AgNO₃ (0.1 mol dm⁻³ in acetonitrile), respectively, potentials were reported with reference to the ferrocenium–ferrocene couple. Elemental analyses were performed by Medac Ltd., Brunel University, UK.

Materials

The preparations of [Au(PPh₃)(NOsO₃)] **1**, *cis*-[Pt-(PMe₃)₂(NOsO₃)₂] **2** and [Au(PPh₃){N(=PPh₃)Ph}][NOsO₃] **7** have been reported previously.[5] The compounds [NBuⁿ₄]-[NOsO₃],[6] *cis*-[Pt(Bupy)₂Cl₂] (Bupy = 4-*tert*-butylpyridine),[7] [Pt(dppm)Cl₂] [dppm = bis(diphenylphosphino)methane],[8] [Ir(CO)(PPh₃)₂Cl],[9] [Rh(cod)(OH₂)(OTs)] (cod = cycloocta-1,5-diene, OTs = tosylate),[10] and [Pt(dppf)Cl₂] [dppf = 1,1′-bis-(diphenylphosphino)ferrocene][11] were synthesised according to the literature methods.

Preparations

***cis*-[Pt(dppm)(NOsO₃)₂] 3.** To a suspension of [Pt(dppm)Cl₂] (0.1 g, 0.15 mmol) in thf (10 cm³) were added 2 equivalents of AgO₃SCF₃ (79 mg, 0.31 mmol) and the resulting mixture was stirred at room temperature overnight and filtered. To the filtrate was added a solution of [NBuⁿ₄][NOsO₃] (0.15 g, 0.3 mmol) in CH₂Cl₂ (5 cm³) and the mixture was stirred for a further hour. The yellow solid was collected and recrystallised from dimethylformamide (dmf)–ether (yield: 0.08 g, 50%). NMR (CDCl₃): ¹H, δ 5.61 (s, 2 H, CH₂) and 7.67–7.99 (m, 20 H, phenyl protons); ³¹P, δ −61.07 (d, ²*J*₍Pt–P₎ 1458 Hz). IR(cm⁻¹): 890 [ν(Os=O)] and 1080 [ν(Os≡N)] (Found: C, 28.2; H, 2.2; N, 2.0. Calc. for C₂₅H₂₂N₂O₆Os₂P₂Pt: C, 27.7; H, 2.0; N, 2.6%).

***trans*-[Pt(Bupy)₂(NOsO₃)₂] 4.** To a suspension of *cis*-[Pt(Bupy)₂Cl₂] (87 mg, 0.16 mmol) in acetone–CH₂Cl₂ (20 cm³,

Table 1 Crystallographic data and experimental details for *trans*-[Pt(Bupy)$_2$(NOsO$_3$)$_2$] **4**, [Ir(CO)(PPh$_3$)$_2$(NOsO$_3$)] **5**, [Au(PPh$_3$){N(=PPh$_3$)-Ph}][NOsO$_3$] **7** and [Pt(dppf)(NOsO$_3$)Cl] **11**

	4	5	7	11
Empirical formula	C$_{18}$H$_{26}$N$_4$O$_6$Os$_2$Pt	C$_{37}$H$_{30}$IrNO$_4$OsP$_2$	C$_{42}$H$_{35}$AuN$_2$O$_3$OsP$_2$	C$_{34}$H$_{28}$ClFeNO$_3$OsP$_2$Pt
M	969.92	997.02	1064.86	1037.14
Crystal system	Triclinic	Monoclinic	Monoclinic	Monoclinic
Space group	$P\bar{1}$ (no. 2)	$P2_1/n$ (no. 14)	$P2_1/n$ (no. 14)	$P2_1/c$ (no. 14)
Colour, habit	Yellow, block	Orange, block	Yellow, plate	Red, block
Crystal dimensions/mm	$0.14 \times 0.18 \times 0.19$	$0.18 \times 0.20 \times 0.25$	$0.12 \times 0.24 \times 0.28$	$0.22 \times 0.22 \times 0.29$
a/Å	7.936(1)	10.124(1)	8.780(1)	20.058(2)
b/Å	10.758(2)	15.564(2)	20.781(2)	14.899(1)
c/Å	7.738(1)	22.623(3)	20.711(5)	23.949(2)
α/°	100.02(1)			
β/°	99.75(1)	100.08(2)	91.23(1)	114.57(2)
γ/°	101.75(1)			
U/Å^3	622.5(2)	3509.7(7)	3778.0(9)	6508(1)
Z	1	4	4	8
D_c/g cm^{-3}	2.587	1.887	1.872	2.117
Diffractometer	Rigaku AFC7R	Enraf-Nonius CAD4	Rigaku AFC7R	MAR-research image plate
T/°C	25.0	25.0	25.0	25.0
λ/Å	0.710 73	0.710 73	0.710 73	0.710 73
Scan type	ω–2θ	ω–2θ	ω–2θ	
$2\theta_{max}$/°	45.0	44.9	45.0	51.3
μ/cm^{-1}	157.95	75.43	73.76	88.19
No. of reflections	1770	5094	5507	12 298
No. of reflections observed [$I > 3.00\sigma(I)$]	1205	3466	3114	6682
Weighting scheme	$1/[\sigma^2(F_o) + 0.005F_o^2/4]$	$1/\sigma^2(F_o)$	$1/[\sigma^2(F_o) + 0.007F_o^2/4]$	$1/\sigma^2(F_o)$
R^a	2.3%	5.4%	3.0%	5.4%
R'^b	2.2%	3.90%	3.0%	7.2%
$F(000)$	440	1896	2040	3920
Goodness of fit^c	1.34	2.46	1.24	2.24

^{a} $R = (\Sigma|F_o| - |F_c|)/\Sigma|F_o|$. ^{b} $R' = [(\Sigma w^2|F_o| - |F_c|)^2/\Sigma w^2|F_o|^2]^{\frac{1}{2}}$. ^{c} Goodness of fit $= [(\Sigma w|F_o| - |F_c|)^2/(N_{observed} - N_{parameters})]^{\frac{1}{2}}$.

1:1) was added to 2 equivalents of AgO$_3$SCF$_3$ (83 mg, 0.32 mmol). The mixture was stirred at room temperature overnight and filtered. To the filtrate was added a solution of [NBu$^n_4$][NOsO$_3$] (0.16 g, 0.32 mmol) in CH$_2$Cl$_2$ (5 cm^3) and the mixture was stirred for 2 h. The solvent was pumped off and the residue recrystallised from CH$_2$Cl$_2$–hexane to give X-ray quality yellow crystals (yield 50 mg, 32%). NMR (CDCl$_3$): ^{1}H, δ 1.37 (s, 9 H, Bu^t), 7.55 (d, 4 H, H$_m$) and 8.38 (d, 4 H, H$_o$). IR(cm^{-1}): 888, 906 [ν(Os=O)] and 1078 [ν(Os≡N)]. UV/VIS (CH$_2$Cl$_2$); λ/nm (ε/dm^3 mol^{-1} cm^{-1}) 352 (14 000), 421 (2890), 437 (2930) and 467 (1540) (Found: C, 22.0; H, 2.7; N, 5.4. Calc. for C$_{18}$H$_{26}$N$_4$O$_6$Os$_2$Pt: C, 22.3; H, 2.7; N, 5.8%).

[Ir(CO)(PPh$_3$)$_2$(NOsO$_3$)] 5. To a suspension of [Ir(CO)(PPh$_3$)$_2$Cl] (0.13 g, 0.17 mmol) in CH$_2$Cl$_2$ (25 cm^3) was added 1 equivalent of AgO$_3$SCF$_3$ (44 mg, 0.17 mmol) and the mixture was stirred for 1 d and filtered. To the filtrate was added a solution of [NBu$^n_4$][NOsO$_3$] (84 mg, 0.17 mmol) in CH$_2$Cl$_2$ (10 cm^3) and the mixture was stirred for a further hour. The solvent was pumped off and the residue recrystallised from CH$_2$Cl$_2$–hexane to give red crystals, which were suitable for an X-ray diffraction study (yield 0.15 g, 90%). NMR (CDCl$_3$): ^{1}H, δ 7.45–7.68 (m, phenyl protons); ^{31}P, δ 27.92 (s). IR(cm^{-1}): 886, 896, 908 [ν(Os=O)], 1098 [ν(Os≡N)] and 1986 [ν(C≡O)]. UV/VIS (CH$_2$Cl$_2$): λ_{max}/nm (ε/dm^3 mol^{-1} cm^{-1}) 350 (5460) (Found: C, 44.6; H, 3.2; N, 1.4. Calc. for C$_{37}$H$_{30}$IrNO$_4$OsP$_2$: C, 44.6; H, 3.0; N, 1.4%).

[{Rh(cod)(NOsO$_3$)}$_2$] 6. To a solution of [Rh(cod)(OH$_2$)(OTs)] (0.1 g, 0.26 mmol) in acetone (10 cm^3) was added 1 equivalent of [NBu$^n_4$][NOsO$_3$] (0.13 g, 0.26 mmol) and the mixture was stirred for 1 h. The brown precipitate was collected, washed with acetone and recrystallised from dmf–diethyl ether (yield 0.17 g, 70%). NMR [(CD$_3$)$_2$SO]: ^{1}H, δ 2.32 (s br, 4 H, CH$_2$), 2.81 (s br, 4 H, CH$_2$) and 4.67 (s br, 4 H, olefinic protons). IR(cm^{-1}): 904 [ν(Os=O)] (Found: C, 21.7, H, 2.8; N, 3.1. Calc. for C$_{16}$H$_{24}$N$_2$O$_6$Os$_2$Rh$_2$: C, 20.7; H, 2.6; N, 3.0%).

[Au(PPh$_3$)(Bupy)][NOsO$_3$] 8. To a solution of [Au(PPh$_3$)(NOsO$_3$)] (71 mg, 0.1 mmol) in CH$_2$Cl$_2$ (10 cm^3) was added 1 equivalent of Bupy (0.015 cm^3, 0.1 mmol) and the mixture

was stirred at room temperature overnight. The solvent was pumped off and the residue was recrystallised from CH$_2$Cl$_2$–hexane to give pale yellow crystals (yield 63 mg, 75%). NMR (CDCl$_3$): ^{1}H, δ 1.34 (s, 9 H, Bu^t), 7.55–7.62 (m, 17 H, aromatic protons) and 8.59 (d, 2 H, H$_o$ or Bupy); ^{31}P, δ 28.5 (s). IR(cm^{-1}): 868, 888 [ν(Os=O)] and 1016 [ν(Os≡N)] (Found: C, 38.1; H, 3.3; N 3.1. Calc. for C$_{27}$H$_{28}$AuN$_2$O$_3$OsP: C, 38.3; H, 3.3; N, 3.3%).

[Pt(dppf)(O$_3$SCF$_3$)$_2$] 9 and [Pt(dppf)(O$_3$SCF$_3$)Cl] 10. To a solution of [Pt(dppf)Cl$_2$] (0.1 g, 0.12 mmol) in CH$_2$Cl$_2$ (10 cm^3) was added 2 equivalents of AgO$_3$SCF$_3$ (63 mg, 0.24 mmol) and the solution was stirred at room temperature overnight. The solvent was pumped off and the residue was recrystallised from CH$_2$Cl$_2$–diethyl ether to give orange and red crystals, which can be separated by inspection or fractional recrystallisation from CH$_2$Cl$_2$–hexane (yield 70 mg). The orange product was identified as the ditriflate [Pt(dppf)(O$_3$SCF$_3$)$_2$]. NMR (CDCl$_3$): ^{1}H, δ 4.49 (s br, 4 H, C$_5$H$_5$), 4.58 (s br, 4 H, C$_5$H$_5$) and 7.48–7.78 (m, 20 H, phenyl protons); ^{31}P, δ 8.04 (t, $^1J_{Pt-P}$ 2102 Hz) (Found: C, 39.4; H, 3.1. Calc. for C$_{36}$H$_{28}$F$_6$FeO$_6$P$_2$PtS$_2$·3H$_2$O: C, 39.2; H, 3.1%).

The red product was identified as the monotriflate [Pt(dppf)(O$_3$SCF$_3$)Cl], which can be synthesised in good yield by reaction of [Pt(dppf)Cl$_2$] with 1 equivalent of AgO$_3$SCF$_3$. NMR (CDCl$_3$): ^{1}H, δ 4.40–4.63 (overlapping s, 8 H, C$_5$H$_5$) and 7.22–7.74 (m, 20 H, phenyl protons); ^{31}P, δ 17.53 (d, $^1J_{Pt-P}$ 1993.5 Hz) (Found: C, 44.2; H, 3.1. Calc. for C$_{35}$H$_{28}$ClF$_3$FeO$_3$P$_2$PtS: C, 45.0; H, 3.0%).

[Pt(dppf)(NOsO$_3$)Cl] 11. To a solution of 9 (0.14 g, 0.15 mmol) in CH$_2$Cl$_2$ (10 cm^3) was added 1 equivalent of [NBu$^n_4$][NOsO$_3$] (74 mg, 0.15 mmol) and the mixture was stirred for 2 h. The solvent was pumped off and the residue recrystallised from CH$_2$Cl$_2$–hexane to give orange crystals (yield 0.14 g, 90%). NMR (CDCl$_3$): ^{1}H, δ 3.99 (s, 1 H, C$_5$H$_5$), 4.37 (s, 1 H, C$_5$H$_5$), 4.56 (s, 2 H, C$_5$H$_5$) and 7.38–7.92 (m, 20 H, phenyl protons); ^{31}P, δ 14.90 (s) and 15.01 (s). IR(cm^{-1}): 888, 908 [ν(Os=O)] and 1096 [ν(Os≡N)]. UV/VIS (CH$_2$Cl$_2$): λ_{max}/nm (ε/dm^3 mol^{-1} cm^{-1}) 322 (7510) (Found: C, 39.3; H, 2.8; N, 1.4. Calc. for C$_{34}$H$_{28}$ClFeNO$_3$OsP$_2$Pt: C, 39.4; H, 2.7; N, 1.4%).
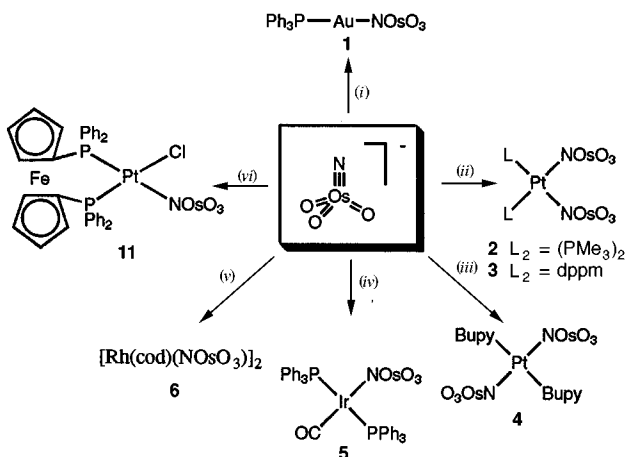
Scheme 1 (*i*) [Au(PPh₃)(O₃SCF₃)]; (*ii*) *cis*-[PtL₂(O₃SCF₃)₂]; (*iii*) *cis*-[Pt(Bupy)₂Cl₂]; (*iv*) [Ir(CO)(PPh₃)₂(O₃SCF₃)]; (*v*) [Rh(cod)(OH₂)(OTs)]; (*vi*) [Pt(dppf)(O₃SCF₃)Cl]

X-Ray crystallography

A summary of crystal data and experimental details for complexes **4**, **5**, **7** and **11** are listed in Table 1. Intensity data were made on a Rigaku AFC7R diffractometer (for **4** and **7**), an Enraf-Nonius CAD4 diffractometer (for **5**), and a MAR research image plate scanner (for **11**) at ambient temperature using graphite-monochromated Mo-Kα radiation (λ 0.710 73 Å). All intensity data were corrected for Lorentz and absorption effects. Semiempirical absorption corrections (ψ scan) were applied for **4**, **5** and **7**. However, no absorption correction was made for **11**. The space group of the crystals was determined by their systematic absences and Laue symmetry. It is noteworthy that for **11** the reported cell data can be transformed into an orthorhombic *C*-centre system. However, the required *mmm* Laue symmetry is absent. The three structures were solved by direct methods and refined on *F* by full-matrix least-squares analysis. Some non-hydrogen atoms were refined anisotropically while the rest were refined isotropically.

Atomic coordinates, thermal parameters, and bond lengths and angles have been deposited at the Cambridge Crystallographic Data Centre (CCDC). See Instructions for Authors, *J. Chem. Soc., Dalton Trans.*, 1997, Issue 1. Any request to the CCDC for this material should quote the full literature citation and the reference number 186/568.

Results and Discussion

Bimetallic nitrido-bridged osmate(VIII) complexes

Bimetallic nitrido-bridged vanadium(v) complexes V≡N–M (M = Rh or Ir) have been previously isolated by Doherty and co-workers[12] from the reaction of X₃V=NSiMe₃ (X = halide) with F–ML₂(CO) (L = PR₃) [equation (1)]. We found that

$$X_3V{=}NSiMe_3 + [F{-}ML_2(CO)] \longrightarrow$$
$$[X_3V{\equiv}N{-}ML_2(CO)] + SiFMe_3 \quad (1)$$
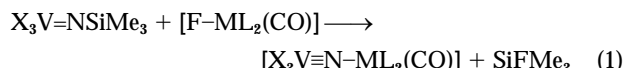
bimetallic nitrido-bridged osmate(VIII) complexes could be prepared conveniently by metathesis of [NOsO₃]⁻ with metal triflates [LₙM(O₃SCF₃)] (M = electrophilic metal) [equation (2)].

$$[NBu^n{}_4][NOsO_3] + [L_nM(O_3SCF_3)] \longrightarrow$$
$$[L_nM{-}N{\equiv}OsO_3] + [NBu^n{}_4][O_3SCF_3] \quad (2)$$
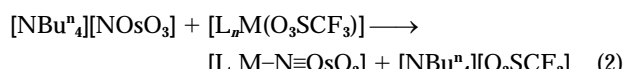
The syntheses of the nitrido-bridged osmate(VIII) complexes are summarised in Scheme 1. The characterisation and crystal structures of [Au(PPh₃)(NOsO₃)] **1** and *cis*-[Pt(PMe₃)₂(NOsO₃)₂] **2**, which were synthesised by the reactions of [NBuⁿ₄][NOsO₃] with [Au(PPh₃)(O₃SCF₃)] and *cis*-[Pt(PMe₃)₂(O₃SCF₃)₂],
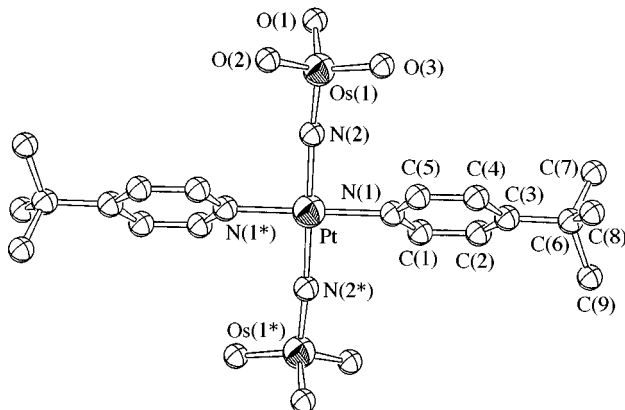
Fig. 1 Perspective view of *trans*-[Pt(Bupy)₂(NOsO₃)₂] **4**
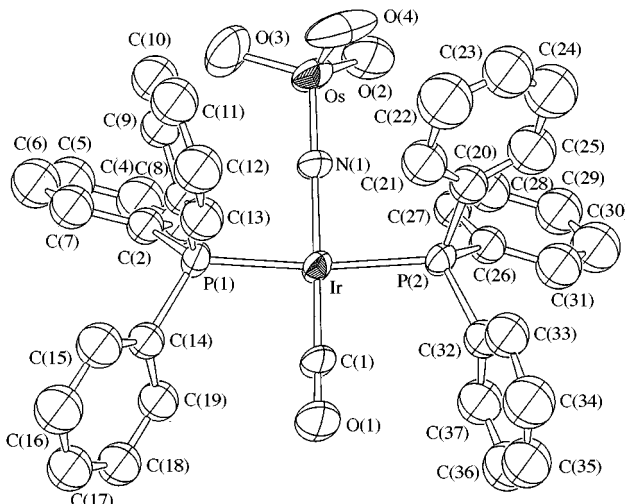
Fig. 2 Perspective view of [Ir(CO)(PPh₃)₂(NOsO₃)] **5**

Table 2 Selected bond lengths (Å) and angles (°) for *trans*-[Pt(Bupy)₂(NOsO₃)₂] **4**

Pt–N(1)	2.040(7)	Pt–N(2)	1.958(7)
Os(1)–O(1)	1.716(7)	Os(1)–O(2)	1.711(8)
Os(1)–O(3)	1.745(8)	Os(1)–N(2)	1.681(7)
N(1)–Pt–N(1*)	180.0	N(1)–Pt–N(2)	89.4(3)
N(1)–Pt–N(2*)	90.6(3)	N(1*)–Pt–N(2)	90.6(3)
N(1*)–Pt–N(2*)	89.4(3)	N(2)–Pt–N(2*)	180.0
O(1)–Os(1)–O(2)	109.9(4)	O(1)–Os(1)–O(3)	111.5(4)
O(1)–Os(1)–N(2)	109.0(4)	O(2)–Os(1)–O(3)	109.2(4)
O(2)–Os(1)–N(2)	108.5(4)	O(3)–Os(1)–N(2)	108.7(4)
Pt–N(2)–Os(1)	172.5(5)		

respectively, have been described previously.[5] Interaction of *cis*-[Pt(dppm)(O₃SCF₃)₂] and *cis*-[Pt(Bupy)₂(O₃SCF₃)₂] with [NOsO₃]⁻ afforded [Pt(dppm)(NOsO₃)₂] **3** and *trans*-[Pt(Bupy)₂(NOsO₃)₂] **4**, respectively. The Os=O and Os≡N stretching frequencies in the IR spectra of complexes **3** and **4** are similar to those found for complex **2**.[5] The structure of **4** has been established by X-ray crystallography. A perspective view of **4** is shown in Fig. 1; selected bond lengths and angles are given in Table 2. The geometry around Pt is square planar with the two [NOsO₃] groups *trans* to each other. The Pt–N (Os) distance of 1.958(7) Å is slightly shorter than those in complexes **2**[5] and **11** (see below) because the *trans* influence for [NOsO₃] is smaller than that for phosphine. The reason why **4** prefers *trans* geometry, which is in contrast to **2**, is not clear. The Os–N and the mean Os–O distances of 1.681(7) and 1.724 Å, respectively, are similar to those for **1** and **2**.

The Vaska-type complex [Ir(CO)(PPh₃)₂(NOsO₃)] **5** was syn-

Table 3 Selected bond lengths (Å) and angles (°) for [Ir(CO)-(PPh₃)₂(NOsO₃)] **5**

Ir–P(1)	2.321(3)	Ir–P(2)	2.327(3)
Ir–N(1)	1.998(7)	Ir–C(1)	1.83(1)
Os–O(2)	1.715(8)	Os–O(3)	1.730(9)
Os–O(4)	1.708(8)	Os–N(1)	1.710(7)
O(1)–C(1)	1.14(1)		
P(1)–Ir–P(2)	169.3(1)	P(1)–Ir–N(1)	87.2(2)
P(1)–Ir–C(1)	92.5(3)	P(2)–Ir–N(1)	88.8(2)
P(2)–Ir–C(1)	91.8(3)	N(1)–Ir–C(1)	177.9(4)
O(2)–Os–O(3)	109.9(4)	O(2)–Os–O(4)	109.3(5)
O(2)–Os–N(1)	108.6(4)	O(3)–Os–O(4)	110.5(4)
O(3)–Os–N(1)	109.2(4)	O(4)–Os–N(1)	108.9(4)
Ir–N(1)–Os	175.5(5)	Ir–C(1)–O(1)	177(1)

Table 4 Selected bond lengths (Å) and angles (°) for [Au(PPh₃)-{N(=PPh₃)Ph}][NOsO₃] **7**

Au–P(2)	2.240(3)	Au–N(1)	2.091(8)
Os–O(1)	1.706(9)	Os–O(2)	1.699(8)
Os–O(3)	1.714(9)	Os–N(2)	1.696(9)
P(1)–N(1)	1.607(9)		
P(2)–Au(1)–N(1)	178.1(2)	O(1)–Os(1)–O(2)	109.8(4)
O(1)–Os(1)–O(3)	108.9(5)	O(1)–Os(1)–N(2)	109.1(6)
O(2)–Os(1)–O(3)	110.1(4)	O(2)–Os(1)–N(2)	109.9(5)
O(3)–Os(1)–N(2)	108.9(5)	Au(1)–N(1)–C(1)	115.7(6)
Au(1)–N(1)–P(1)	115.6(5)	P(1)–N(1)–C(1)	127.0(7)

I
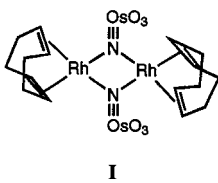
thesised by the reaction of [Ir(CO)(PPh₃)₂(O₃SCF₃)] with [NOsO₃]⁻, isolated as air-stable red crystals. Fig. 2 shows a diagram of the molecule; selected bond lengths and angles are given in Table 3. As expected the geometry around Ir is square planar with the [NOsO₃] group *trans* to the carbonyl. The Ir–P, Ir–C and Ir–N distances are normal by comparison with the isostructural iridium(I)–amide complex [Ir(CO)(PPh₃)₂(3,5-Me₂C₆H₃NH)].[13] The short Os–N distance [1.710(7) Å] and long Ir–N bond [1.998(7) Å] is suggestive of the unsymmetric bridging mode of the nitride, *i.e.* Ir–N≡Os. The ν(C=O) for **5** was found at 1986 cm⁻¹, which is lower than that for [Ir(CO)(PPh₃)₂(3,5-Me₂C₆H₃NH)] (1941 cm⁻¹)[13] and [Ir(CO)-(PPh₃)₂(CO)] (1965 cm⁻¹), indicating that [NOsO₃]⁻ is a weak donor ligand. On the basis of the CO stretching frequency, the donor strength of [NOsO₃]⁻ is considered comparable to that of a nitrite (1987 cm⁻¹).[14]

Reaction of [Pt(cod)(O₃SCF₃)₂] and 'Ir(cod)(O₃SCF₃)', which were prepared *in situ* from [Pt(cod)Cl₂] and [{Ir(cod)Cl}₂], respectively, with [NOsO₃]⁻ led to isolation of uncharacterised insoluble brown solids. On the other hand, treatment of [Rh-(cod)(OH₂)(OTs)] with [NOsO₃]⁻ gave a well defined solid analysed as [Rh(cod)(NOsO₃)] **6**. This solid is insoluble in chlorinated solvents but readily dissolves in dmf and dimethyl sulfoxide. The ¹H NMR spectrum of **6** shows signals characteristic of co-ordinated cod. In addition, the IR spectrum shows that ν(Os=O) and ν(Os≡N) are shifted to higher frequency, indicating that the [NOsO₃] moiety in **6** is co-ordinated rather than a counter anion. Unfortunately, we were not able to obtain X-ray quality crystals for **6** due to its poor solubilities in common organic solvents. We tentatively formulate **6** as a NOsO₃-bridged dirhodium(I) complex [{Rh(cod)}₂(μ-NOsO₃)₂], which is the first example of a complex with a bridging [NOsO₃] ligand.

Reactivities of bimetallic nitrido-bridged complexes

In an attempt to synthesise an imido(nitrido)osmium(VIII) complex *via* oxo–imido exchange, we tried the reaction of complex **1** with phosphinimine. Treatment of **1** with PhN=PPh₃ resulted in substitution of the phosphinimine for [NOsO₃], instead of the oxo–imido exchange. The product was characterised as [Au(PPh₃){N(=PPh₃)Ph}][NOsO₃] **7** by X-ray crystallography. Fig. 3 shows a perspective view of the molecule; selected bond lengths and angles are given in Table 4. The P–Au–N linkage is essentially linear while the C–N=P angle in

Fig. 3 Perspective view of [Au(PPh₃){N(=PPh₃)Ph}][NOsO₃] **7**

the phosphinimine is 127.0(7)°. The Au^I–N distance is similar to that in **1**.[4] There is no interaction of the Au centre with the osmate, which is essentially a counter anion.

In contrast to the imido(trioxo)osmium(VIII) complexes, no reactions of complexes **1–4** with alkenes were observed. In an attempt to activate these osmate(VIII) complexes by Lewis base complexation, or so-called 'ligand acceleration',[15] we tried the reactions of **1** with alkenes in the presence of pyridine. Treatment of dimethylbut-2-ene with stoichiometric amounts of complex **1** and 4-*tert*-butylpyridine (Bupy) led to isolation of an adduct analysed as **1·**Bupy **8**. No cycloaddition reaction of **1** with dimethylbut-2-ene occurred, as evidenced by ¹H and ¹³C NMR spectroscopy. Complex **8** was, however, incorrectly formulated as the osmium–pyridine adduct [OsO₃{NAu(PPh₃)}-Bupy] in the previous communication.[5] The correct structure for **8** should be [Au(PPh₃)(Bupy)][NOsO₃] because the Os=O and Os≡N stretching frequencies for **8** are close to the values for **7**, in which the [NOsO₃] moiety is a counter anion. The [NOsO₃] group in **1** is quite labile and can be displaced easily apparently because the Au–N bond is weak.

Similar to Vaska complexes, **5** was found to undergo oxidative addition with MeI. The IR spectrum of the crude product, presumably [Ir(CO)(PPh₃)(Me)(NOsO₃)I], shows a ν(C≡O) stretch at 2010 cm⁻¹, which is typical for Ir^III complexes.[14,16] However, the ¹H and ³¹P-{¹H} NMR spectra show that the crude product consists of three isomers, which have yet to be separated.

Trimetallic complexes

In the hope of activating the [NOsO₃] group by intramolecular electron transfer, trioxoosmium(VIII) complexes containing the redox-active dppf ligand were synthesised. Metathesis of [Pt(dppf)Cl₂] with 2 equivalents of AgO₃SCF₃ led to the
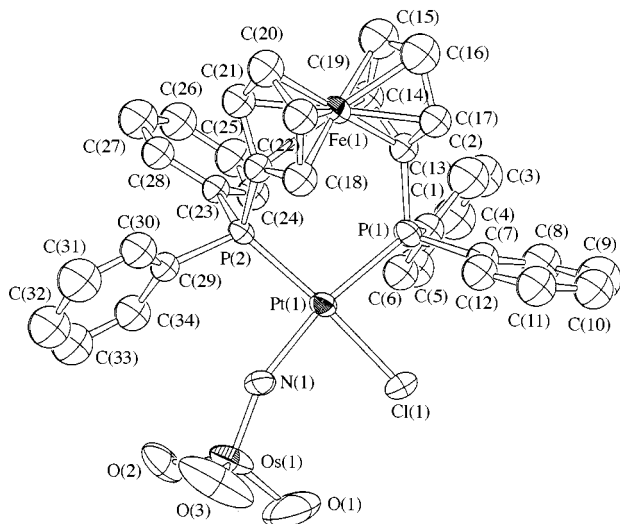
Fig. 4 Perspective view of one of the two independent molecules in the unit cell for [Pt(dppf)(NOsO$_3$)Cl] 11

Table 5 Selected bond lengths (Å) and angles (°) for [Pt(dppf)-(NOsO$_3$)Cl] 11

Pt(1)–Cl	2.317(5)	Pt(1)–P(1)	2.269(4)
Pt(1)–P(2)	2.265(5)	Pt(1)–N(1)	2.05(1)
Os(1)–O(1)	1.77(2)	Os(1)–O(2)	1.69(1)
Os(1)–O(3)	1.69(2)	Os(1)–N(1)	1.66(1)
Pt(2)–Cl(1)	2.354(6)	Pt(2)–P(3)	2.250(5)
Pt(2)–P(4)	2.287(5)	Pt(2)–N(2)	2.06(2)
Os(2)–O(4)	1.66(2)	Os(2)–O(5)	1.68(2)
Os(2)–O(6)	1.53(2)	Os(2)–N(2)	1.65(2)
Cl(1)–Pt(1)–P(1)	85.0(2)	Cl(1)–Pt(1)–P(2)	175.4(2)
Cl(1)–Pt(1)–N(1)	83.5(4)	P(1)–Pt(1)–P(2)	99.6(2)
P(1)–Pt(1)–N(1)	168.1(4)	P(2)–Pt(1)–N(1)	91.9(4)
O(1)–Os(1)–O(2)	108.7(8)	O(1)–Os(1)–O(3)	112(1)
O(1)–Os(1)–N(1)	108.1(9)	O(2)–Os(1)–O(3)	111.3(9)
O(2)–Os(1)–N(1)	109.6(7)	O(3)–Os(1)–N(1)	106.4(9)
Pt(1)–N(1)–Os(1)	160.4(9)	Cl(2)–Pt(2)–P(3)	174.6(2)
Cl(2)–Pt(2)–P(4)	87.7(2)	P(3)–Pt(2)–P(4)	97.7(2)
P(3)–Pt(2)–N(2)	90.4(5)	P(4)–Pt(2)–N(2)	171.8(5)
O(4)–Os(2)–O(5)	111(1)	O(4)–Os(2)–O(6)	107.1
O(4)–Os(2)–N(2)	110.6(8)	O(5)–Os(2)–O(6)	116(1)
Os(5)–Os(2)–N(2)	107.1(8)	O(6)–Os(2)–N(2)	103(1)
Pt(2)–N(2)–Os(2)	152(1)		

isolation of a mixture of orange ditriflate [Pt(dppf)(O$_3$SCF$_3$)$_2$] 9 and red monotriflate [Pt(dppf)(O$_3$SCF$_3$)Cl] 10, which can be separated by inspection or fractional crystallisation. Reaction of [Pt(dppf)Cl$_2$] with 1 equivalent of AgO$_3$SCF$_3$, however, gave the monotriflate as the major product. Treatment of 10 with [NOsO$_3$]$^-$ resulted in the formation of the trimetallic Fe^{II}–Pt^{II}–Os^{VIII} complex [Pt(dppf)(NOsO$_3$)Cl] 11, the structure of which has been confirmed by X-ray diffraction. Fig. 4 shows a perspective view of one of the two independent molecules in the unit cell; selected bond lengths and angles are given in Table 5. As expected, the geometry around Pt is square planar. The mean Pt–P and Pt–Cl bond distances in 11 are similar to those for [Pt(dppf)Cl$_2$].[10] The mean Os–N and Os–O distances of 1.66 and 1.67 Å, respectively, are normal compared with other osmate(VIII) complexes. Interestingly, the Pt–N≡Os linkage in 11 is found to be slightly bent with an average angle of *ca.* 156.2°, this bending is attributed to the non-bonding repulsion between the NOsO$_3$ group and the phenyl ring of dppf.

Electrochemical studies

Table 6 summarises the electrochemical data for the nitrido-bridged osmate(VIII) complexes. The cyclic voltammogram of complex 4 shows an irreversible reduction wave at *ca.* −1.23 V
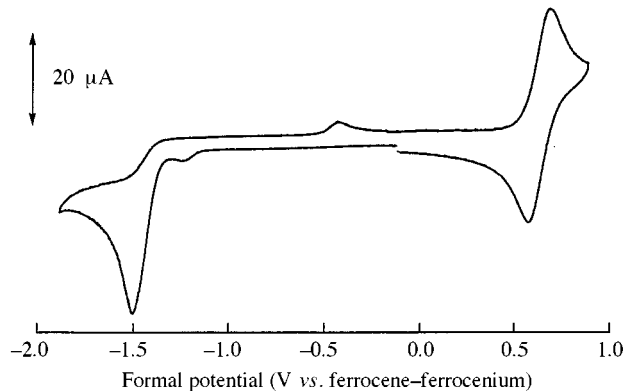

Fig. 5 Cyclic voltammogram of [Pt(dppf)(NOsO$_3$)Cl]. Supporting electrolyte: 0.1 mol dm^{-3} NBu$^n_4$PF$_6$ in CH$_2$Cl$_2$; working electrode glassy carbon; scan rate 100 mV s^{-1}

Table 6 Formal electrode potentials ($E°$) for nitrido-bridged osmate-(VIII) complexes[a]

	$E°$/V *vs.* ferrocene–ferrocenium	
Compound	Oxidation	Reduction
[NOsO$_3$]$^-$		−1.45[b]
[Au(PPh$_3$)(NOsO$_3$)]		−1.31[b]
[Pt(Bupy)$_2$Cl$_2$]		−2.13[b]
trans-[Pt(Bupy)$_2$(NOsO$_3$)$_2$]		−1.23[b]
[Pt(dppf)Cl$_2$]	0.56	−2.13[b]
[Pt(dppf)(O$_3$SCF$_3$)$_2$]	0.86	−1.34[b]
[Pt(dppf)(NOsO$_3$)Cl]	0.67	−1.50[b]
[Ir(CO)(PPh$_3$)$_2$(NOsO$_3$)]		−1.67[b]
[Os(NBu^t)O$_3$]	0.92	

[a] Supporting electrolyte: 0.1 mol dm^{-3} NBu$^n_4$PF$_6$ in CH$_2$Cl$_2$; working electrode glassy carbon; scan rate = 100 mV s^{-1}. [b] Irreversible, E_{pc} values.

vs. Cp$_2$Fe$^{+/0}$ (Cp = η^5-C$_5$H$_5$). This reduction wave is tentatively attributed to the Os^{VIII}–Os^{VII} reduction because the Pt-centred reduction for *cis*-[Pt(Bupy)$_2$Cl$_2$] was found at a more negative potential (*ca.* −2.13 V). The reduction of Os^{VIII} in 4 occurs at a less negative potential than that in [NOsO$_3$]$^-$ (*ca.* −1.45 V under the same conditions), suggestive of delocalisation of electrons from [NOsO$_3$] to Pt^{II} in complex 5.

The cyclic voltammogram of complex 11 (Fig. 5) shows a reversible couple at 0.67 V (ΔE_p = 80 mV, $i_a/i_c \approx 1$ and is scan rate independent) along with an irreversible reduction wave at −1.50 V *vs.* Cp$_2$Fe$^{+/0}$. The oxidation couple is assigned as the ferrocene-centred Fe^{III}–Fe^{II} couple. However, it seems that this oxidation couple might also have some Pt^{III}–Pt^{II} character because the oxidation potential for the [Pt(dppf)X$_2$] complexes shows a dependence on the nature of X. It decreases from [Pt(dppf)(O$_3$SCF$_3$)$_2$] (0.866 V), [Pt(dppf)(NOsO$_3$)Cl] (0.67 V) to [Pt(dppf)Cl$_2$] (0.56 V). This order is consistent with the trend of donor strength of X: Cl > NOsO$_3$ > O$_3$SCF$_3$. The irreversible wave at −1.50 V in 11 is tentatively assigned as the osmium-centred reduction because the reduction of Pt^{II} for [Pt(dppf)-Cl$_2$] was found at a very negative potential (*ca.* −2.13 V).

The cyclic voltammogram of complex 5 shows an irreversible reduction wave at −1.67 V *vs.* Cp$_2$Fe$^{+/0}$. This was tentatively attributed to the reduction of Os^{VIII}–Os^{VII} because the iridium-centred reductions for Vaska-type compounds are known to occur at more negative potentials (< −2.00 V *vs.* Ag$^+$–Ag).[14] On the basis of the potential at which Os^{VIII} in [L$_n$M–NOsO$_3$] is reduced, the donor strength of the fragment L$_n$M can be ranked in the order {Ir^I(CO)(PPh$_3$)$_2$} > {Au^I(PPh$_3$)} > {Pt^{II}(Bupy)$_2$}. This trend is in agreement with the order of electron-withdrawing power of the metal centre: Ir^I < Au^I < Pt^{II}. It might also be noted that the Os^{VIII}–Os^{VII} reduction potential for [Os(NBu^t)O$_3$] is found to be less negative than those for

Table 7 Structural and IR spectral data for nitrido-bridged osmate(VIII) complexes

Complex	$d(\text{Os}{\equiv}\text{N})/\text{Å}$	$d(\text{Os}{=}\text{O})/\text{Å}$	$\nu(\text{Os}{\equiv}\text{N})/\text{cm}^{-1}$	$\nu(\text{Os}{=}\text{O})/\text{cm}^{-1}$
$[\text{NOsO}_3]^{-\,a}$	1.67(2)	1.744(1)	1073	891, 871
$[\text{NOsO}_3]^{-}$ in **7**	1.696(9)	1.706(9)	1104	888
$[\text{Au(PPh}_3)(\text{NOsO}_3)]^{\,b}$	1.69(2)	1.71	1088	894
cis-$[\text{Pt(PMe}_3)_2(\text{NOsO}_3)_2]^{\,b}$	1.68(4)	1.76	1088	894
trans-$[\text{Pt(Bupy)}_2(\text{NOsO}_3)_2]$	1.681(7)	1.724	1078	888, 906
$[\text{Pt(dppf)(NOsO}_3)\text{Cl}]$	1.655(1)	1.67	1096	888, 908
$[\text{Ir(CO)(PPh}_3)_2(\text{NOsO}_3)]$	1.710(7)	1.718	1098	886, 896, 908
$[\{\text{Rh(cod)}\}_2(\mu\text{-NOsO}_3)_2]$				904
$[\text{Os(NBu}^t)\text{O}_3]^{\,c}$	1.697	1.715	1184	912, 925

a Structural data for Cs[NOsO$_3$], Raman spectrum of aqueous K[NOsO$_3$] (ref. 17). *b* Ref. 5. *c* Ref. 18.

$[\text{L}_n\text{M}{-}\text{N}{\equiv}\text{OsO}_3]$, indicating that the donor strength of nitride is significantly reduced upon formation of a C–N covalent bond.

Structural and IR spectral data for osmate(VIII) complexes

Table 7 summarises the structural and IR spectra data for the nitrido-bridged osmate(VIII) complexes $[\text{L}_n\text{M}{-}\text{N}{\equiv}\text{OsO}_3]$. It appears that neither the Os≡N nor the Os=O distances for these complexes are significantly changed upon co-ordination to the metal (M) despite the large estimated standard deviation (e.s.d.) values for these structural data. In all cases, the Os≡N–M linkage is linear with an Os≡N triple bond and an M–N single bond. This suggests that these bimetallic complexes are best formulated as the unsymmetrically nitrido-bridged complexes $[\text{L}_n\text{M}{-}\text{N}{\equiv}\text{OsO}_3]$.[19] Unlike imido(trioxo)osmium(VIII) complexes $[\text{Os(NR)O}_3]$, the M–N bond in $[\text{L}_n\text{M}{-}\text{N}{\equiv}\text{OsO}_3]$ is of donor–acceptor type only and is rather weak. Accordingly, the $[\text{NOsO}_3]$ group in these complexes is found to be substitution labile.

The IR stretching frequency is found to be more sensitive than the bond length to the change in bond strength. In general, $\nu(\text{Os}{\equiv}\text{N})$ for $[\text{NOsO}_3]$ increases upon co-ordination to metal. A similar observation has been reported for the complexation of Lewis acids with $[\text{Re(N)Br}_4]^{-}$.[20] The strengthening of the Os≡N bond in $[\text{NOsO}_3]^{-}$ upon metal complexation may be explained by the fact that the lone pair on the nitride has anti-bonding character. In addition, $\nu(\text{Os}{=}\text{O})$ for $[\text{L}_n\text{M}{-}\text{N}{\equiv}\text{OsO}_3]$ complexes are found to be higher than those for $[\text{NOsO}_3]^{-}$, indicating that the donor strength of the nitride is weakened upon co-ordination to metal. For $[\text{L}_n\text{M}{-}\text{N}{\equiv}\text{OsO}_3]$ $\nu(\text{Os}{=}\text{O})$ is, however, lower than that for $[\text{Os(NR)O}_3]$ (Table 7) because the donor–acceptor type M–N bond is weaker than a C–N covalent bond. On the basis of $\nu(\text{Os}{=}\text{O})$ it can be concluded that the donor strength for NX in $[\text{Os(NX)O}_3]$ decreases in the order $\text{N}^{3-} > (\text{L}_n\text{MN})^{2-} > \text{RN}^{2-}$, which is consistent with the electrochemical data (see above). The complexes $[\text{L}_n\text{M}{-}\text{N}{\equiv}\text{OsO}_3]$ are less reactive than $[\text{Os(NR)O}_3]$, *e.g.* in cycloaddition reactions with alkenes,[2] possibly because the former complexes are more electron-rich and thus less electrophilic than the latter.

References

1 R. Criegee, *Justus Liebigs Ann. Chem.*, 1936, **522**, 75; M. Schröder, *Chem. Rev.*, 1980, **80**, 107 and refs. therein; W. B. Motherwell and A. S. Williams, *Angew. Chem., Int. Ed. Engl.*, 1995, **34**, 2031.
2 K. B. Sharpless, D. W. Patrick, L. K. Truesdale and S. A. Biller, *J. Am. Chem. Soc.*, 1975, **97**, 2305; K. B. Sharpless, A. O. Chong and K. Oshima, *J. Org. Chem.*, 1976, **41**, 177.
3 H. C. Holb, M. S. VanNieuwenhze and K. B. Sharpless, *Chem. Rev.*, 1994, **94**, 2483 and refs. therein.
4 G. Liu, H. T. Chang and K. B. Sharpless, *Angew. Chem., Int. Ed. Engl.*, 1996, **35**, 45; J. Rudolph, P. C. Sennhenn, C. P. Vlaar and K. B. Sharpless, *Angew. Chem., Int. Ed. Engl.*, 1996, **35**, 2810; G. Li, H. H. Angert and K. B. Sharpless, *Angew. Chem., Int. Ed. Engl.*, 1996, **35**, 2813.
5 W.-H. Leung, J. L. C. Chim and W.-T. Wong, *J. Chem. Soc., Dalton Trans.*, 1996, 3153.
6 A. F. Clifford and C. S. Kobayashi, *Inorg. Synth.*, 1960, **6**, 204.
7 G. B. Kauffamn, *Inorg. Synth.*, 1963, **7**, 249.
8 M. P. Brown, R. J. Puddephatt, M. Rashidi and K. R. Seddon, *J. Chem. Soc., Dalton Trans.*, 1977, 951.
9 J. P. Collman and M. Kubota, *Inorg. Synth.*, 1990, **28**, 92.
10 U. Kölle, R. Görissen and T. Wagner, *Chem. Ber.*, 1995, **128**, 911.
11 D. A. Clemente, G. Pilloni, B. Corain, B. Longato and M. Tiripicchio-Camellini, *Inorg. Chim. Acta*, 1986, **115**, L9.
12 N. W. Hoffman, N. Prokopuk, M. J. Robbins, C. M. Jones and N. M. Doherty, *Inorg. Chem.*, 1991, **30**, 4177.
13 M. Rahim and K. J. Ahmed, *Organometallics*, 1994, **13**, 1751.
14 G. J. Leigh and R. L. Richards, in *Comprehensive Organometallic Chemistry*, eds. G. Wilkinson, F. G. A. Stone and E. W. Abel, Pergamon, Oxford, vol. 5, p. 543.
15 D. J. Berrisford, C. Bolm and K. B. Sharpless, *Angew. Chem., Int. Ed. Engl.*, 1995, **34**, 1059.
16 C. A. Reed and W. R. Roper, *J. Chem. Soc., Dalton Trans.*, 1973, 1370.
17 W. A. Nugent and J. M. Mayer, *Metal-Ligand Multiple Bonds*, Wiley, New York, 1988, p. 126.
18 B. S. McGilligan, J. Arnold, G. Wilkinson, B. Hussain-Bates and M. B. Hursthouse, *J. Chem. Soc., Dalton Trans.*, 1990, 2465.
19 K. Dehnicke and J. Strähle, *Angew. Chem., Int. Ed. Engl.*, 1992, **31**, 955.
20 W. Kafitz, F. Weller and K. Dehnicke, *Z. Anorg. Allg. Chem.*, 1982, **590**, 175.